

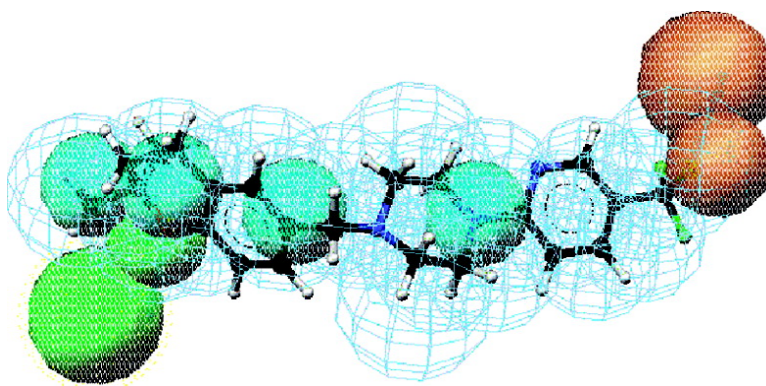
Article

**Pharmacophore Modeling, Docking, and Principal Component Analysis  
Based Clustering: Combined Computer-Assisted Approaches  
To Identify New Inhibitors of the Human Rhinovirus Coat Protein**

Theodora M. Steindl, Carolyn E. Crump, Frederick G. Hayden, and Thierry Langer

*J. Med. Chem.*, **2005**, 48 (20), 6250-6260 • DOI: 10.1021/jm050343d • Publication Date (Web): 02 September 2005

Downloaded from <http://pubs.acs.org> on March 28, 2009



**More About This Article**

Additional resources and features associated with this article are available within the HTML version:

- Supporting Information
- Links to the 7 articles that cite this article, as of the time of this article download
- Access to high resolution figures
- Links to articles and content related to this article
- Copyright permission to reproduce figures and/or text from this article

[View the Full Text HTML](#)

# Pharmacophore Modeling, Docking, and Principal Component Analysis Based Clustering: Combined Computer-Assisted Approaches To Identify New Inhibitors of the Human Rhinovirus Coat Protein<sup>§</sup>

Theodora M. Steindl,<sup>†</sup> Carolyn E. Crump,<sup>‡</sup> Frederick G. Hayden,<sup>‡</sup> and Thierry Langer<sup>\*,†</sup>

Department of Pharmaceutical Chemistry, Institute of Pharmacy, and Center for Molecular Biosciences Innsbruck (CMBI), University of Innsbruck, Innrain 52c, A-6020 Innsbruck, Austria, and Department of Internal Medicine, University of Virginia School of Medicine, Box 473, Charlottesville, Virginia 22908

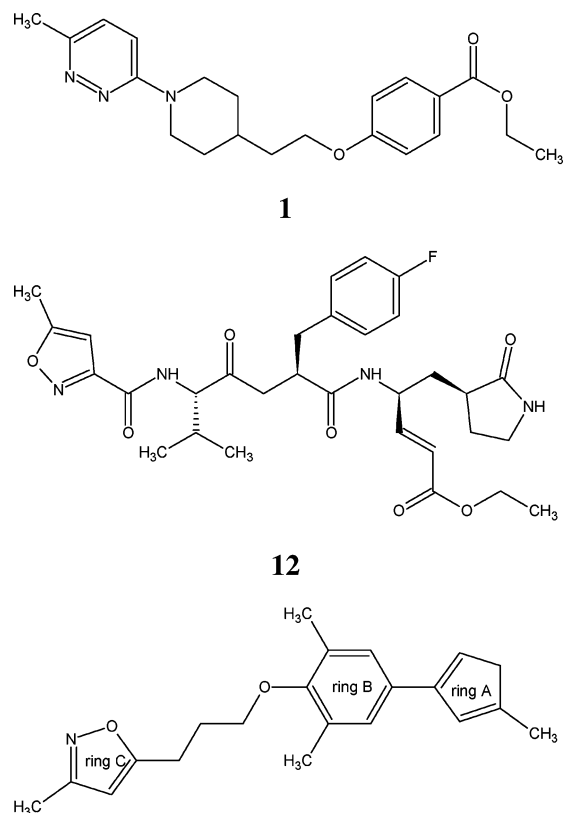
Received April 13, 2005

The development and application of a sophisticated virtual screening and selection protocol to identify potential, novel inhibitors of the human rhinovirus coat protein employing various computer-assisted strategies are described. A large commercially available database of compounds was screened using a highly selective, structure-based pharmacophore model generated with the program Catalyst. A docking study and a principal component analysis were carried out within the software package Cerius<sup>2</sup> and served to validate and further refine the obtained results. These combined efforts led to the selection of six candidate structures, for which in vitro antirhinoviral activity could be shown in a biological assay.

## Introduction

The human rhinovirus (HRV) belongs to the family of picornaviruses and is the main cause for common colds and a variety of other respiratory illnesses including otitis media, sinusitis, and exacerbations of asthma and reactive airways disease. These illnesses still lack effective antiviral treatment. The viral capsid is a promising and intensively studied target for drug development. This protein shell encapsulates a single, positive RNA strand and consists of 60 copies of four different viral proteins. More than 100 HRV serotypes are known to date and are classified as major receptor group viruses, like serotypes 3, 14, 16, and 39 that utilize intercellular adhesion molecule-1 (ICAM-1) as cellular receptor, and as minor receptor group viruses, which use members of the low-density lipoprotein receptor family to attach to cells. Examples for the latter group are serotypes 1A and 2. HRV coat protein inhibitors act as capsid-binding antiviral agents that block the uncoating of the viral particles and/or inhibit cell attachment.<sup>1</sup> Their binding site is located within a hydrophobic pocket situated at the bottom of a depression, a so-called canyon, on the capsid surface. In the absence of an inhibitor, this pocket can be empty or occupied by a pocket factor, a lipid or fatty acid. Structural conservation in this region among the different serotypes permits the development of broad-spectrum anti-HRV agents.<sup>1,2</sup> Natural products as well as synthetic compounds interacting with the capsid of picornaviruses have been known for a long time, and

**Chart 1.** Chemical Structures of a Broad-Spectrum Anticoronavirus Coat Protein Inhibitor (Top) and a HRV 3C Protease Inhibitor (Middle) and General Design of WIN Compounds (Bottom)



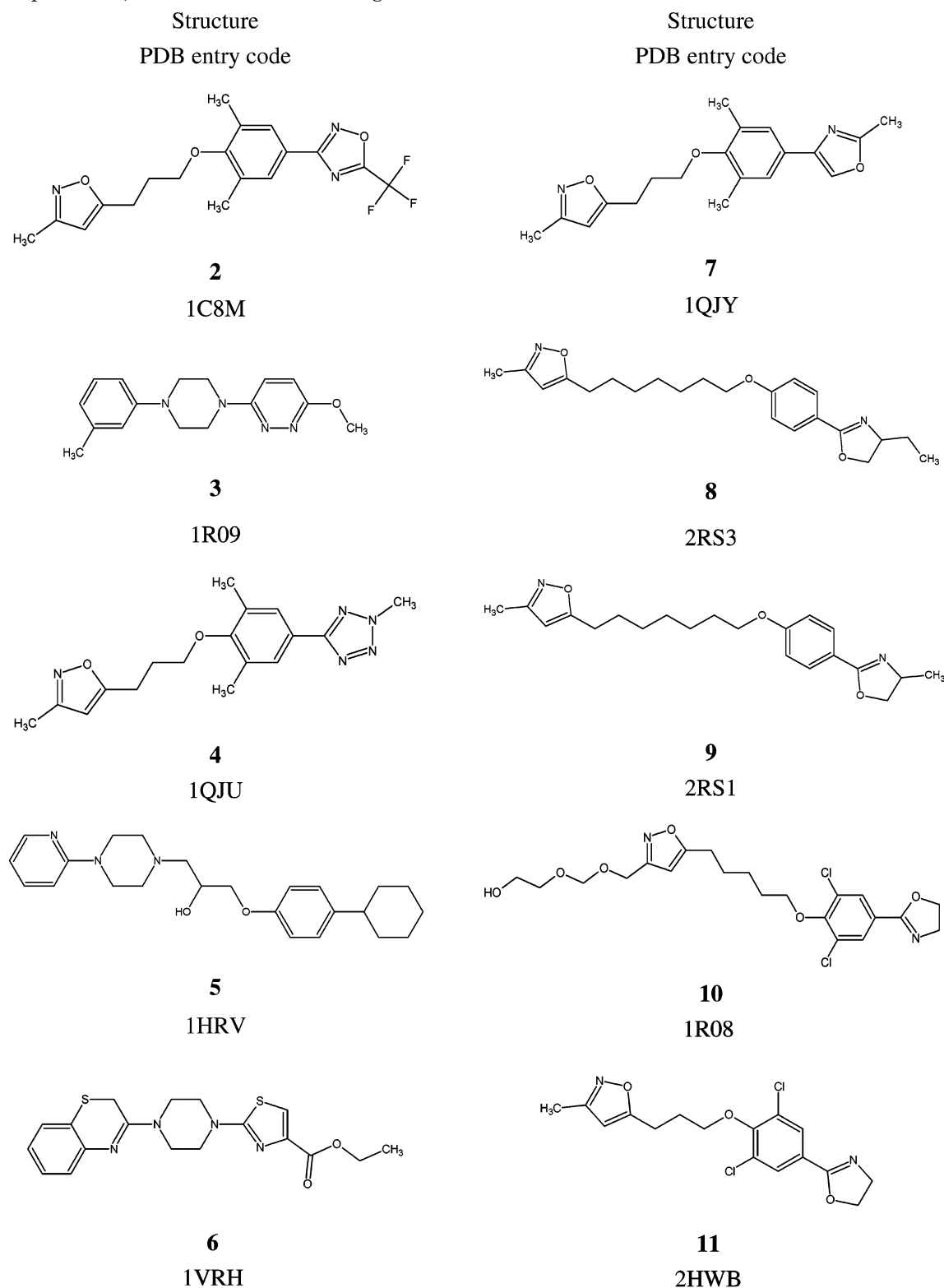
<sup>§</sup> Parts of this study have been presented at the 18th Darmstädter Molecular Modelling Workshop, May 18–19, 2004, Erlangen, Germany, and at the 18th International Symposium on Medicinal Chemistry (ISMC), August 15–19, 2004, Kopenhagen-Malmö, Denmark, Sweden, as oral presentations and at the 15th European Symposium on Quantitative Structure–Activity Relationships & Molecular Modelling, September 5–10, 2004, Istanbul, Turkey, as poster presentations.

\* To whom correspondence should be addressed. Phone: +43 512 507 5252. Fax: +43 512 507 5269. E-mail: thierry.langer@uibk.ac.at.

<sup>†</sup> University of Innsbruck.

<sup>‡</sup> University of Virginia School of Medicine.

several, specifically pirodavir (**1**) (Chart 1) and pleconaril (**2**) (Chart 2),<sup>3,4</sup> have undergone advanced clinical testing. A more detailed investigation of the molecular basis for the antiviral activity of these compounds and the systematic search for novel, even more active structures was enabled when X-ray crystallographic structure information on the protein became available.<sup>5</sup>

**Chart 2.** Structures of 10 Known HRV Coat Protein Inhibitors Used for Pharmacophore Model Generation, HTVS Docking Experiments, and PCA-Based Clustering

Nowadays, the Brookhaven Protein Databank (PDB)<sup>6</sup> contains about 30 entries of the HRV coat protein in complex with an inhibitor. In our study we took advantage of these sources for the generation of the pharmacophore models and for setup of the docking process.

In the rational drug development process many computer-assisted techniques have emerged to increase efficiency in the search for new leads.<sup>7</sup> A reduction of time and costs for biological assays can be achieved by

checking the likeliness of a substance to exhibit activity at the target of interest beforehand. In the present study, we apply a combined approach of virtual screening techniques (pharmacophore model generation, docking, and ligand clustering in combination with a principal component analysis (PCA) performed on a set of molecular descriptors) to select a small set of possible new HRV coat protein inhibitors from a large commercially available database (DB). A pharmacophore

model defines a special arrangement of chemical features that are shared by different ligands and are obviously responsible for binding and, as a consequence, for biological activity.<sup>8</sup> Such a model can be used as query tool in 3D DB mining, thereby provoking an enrichment of active compounds in the obtained hit lists. Using the crystal structure of an inhibitor complexed with the HRV coat protein and the functional group definitions contained within the Catalyst software,<sup>9</sup> a representation of the binding site was produced (structure-based pharmacophore model) and applied in screening the commercially available Maybridge DB.<sup>10</sup> The resulting hits were submitted to further investigations using a docking study as well as a PCA of a set of molecular descriptors, thus aiming at the final selection of few compounds for biological testing. Docking utilizes the crystal structure of a target protein and calculates different binding modes for the structures of interest. Application of a scoring function (SF) allows the estimation of binding affinities and therefore a ranking of the substances. PCA is a widely applied multivariate technique in drug discovery. It provides a reduction of data multidimensionality (i.e., the properties of the input molecules), gives an overview of the data, and detects trends, groupings, and outliers.<sup>11</sup> In our study PCA-based clustering was applied to estimate the similarity of the Maybridge hits with already known active molecules. The docking and scoring procedures as well as the PCA-based clustering were carried out within the Cerius<sup>2</sup> software.<sup>12</sup> The combination of pharmacophore model generation, docking, and PCA-based clustering presents a virtual screening and selection protocol aimed at the fast and reliable identification of potential new HRV coat protein inhibitors. Thereby each step underwent thorough theoretical validation probing their performance on sets of known active and by all probability inactive compounds.

These combined efforts finally allowed the selection of six promising candidate structures that were tested in a biological assay exemplarily against one major receptor group virus serotype for in vitro anti-HRV activities. The promising results of this biological testing were considered as a further proof of concept for our workflow.

## General Methodology

**Binding Site Analysis, Catalyst Pharmacophore Model Generation, and Database Screening.** The program Catalyst allows the generation of pharmacophore models, also termed hypotheses. A Catalyst pharmacophore model consists of a 3D arrangement of a collection of features necessary for the biological activity of the ligands. Whereas some features (like hydrogen bond acceptor (HBA) or hydrogen bond donor (HBD)) are defined as vectors, others (for example, hydrophobic (H) features) are located at centroids of the corresponding (e.g., hydrophobic) ligand atoms. The features in Catalyst are associated with location constraints, displayed as colored spheres, which allow a certain spherical tolerance surrounding the ideal position of a particular feature in 3D space.

Catalyst models may be used as queries to search 3D coordinate DBs of organic molecules for structurally new, potentially bioactive ligands. To be retrieved as a

hit, a molecule must possess appropriate functional groups that match the features of the pharmacophore model. An automatic pharmacophore generation process in Catalyst requires the input of several active ligands that share the same binding mode. Depending on the properties and information content of these training set molecules, qualitative or quantitative hypotheses may be generated. Alternatively, the features of the pharmacophore may be placed manually, guided by the X-ray structure of a receptor–ligand complex. In the present study the latter, so-called structure-based approach, was used.

Crystal structure files of HRV coat protein in complex with an inhibitor present in the PDB were studied, and several important pharmacophore features could be identified. All inhibitors possess a rather hydrophobic character to match the lipophilic environment of this binding site. For the pharmacophore model generation this implies the inclusion of several hydrophobic features. Another characteristic is the tendency of many ligands to form hydrogen bonds to the amide nitrogen of Leu 100,<sup>1</sup> situated at the heel of the pocket, which was taken into account by an HBA.<sup>13</sup> A possibility for electrostatic interaction in a hydrophilic area at the innermost part of the site can be given by some but not all of the ligands. In the resulting hypothesis, the introduction of this feature provokes an increase in selectivity. Since the protein imposes strict steric requirements on ligand binding, it is tremendously important for a new ligand that it fits the spatial restrictions of this approximately 20 Å long tunnel-shaped pocket. Excluded volume spheres and the generation of a shape, as was performed in this study, are the solutions within Catalyst to account for these dimensional borderlines of the protein.

The next step was the application of the generated hypotheses in 3D DB screening. A valuable hypothesis should identify as many of the known inhibitors and as few false positives as possible from a DB. If only a certain number of compounds from a hit list can be selected for purchase and biological assay, a longer hit list will be avoided because it generates larger time and cost expenses for the postprocessing involved. To validate the quality of the hypotheses generated within this study, an internal inhibitor DB, the so-called test set, consisting of 22 HRV coat protein inhibitors belonging to different structural classes and the Derwent WDI,<sup>14</sup> which contains approximately 50 000 biologically active compounds, were screened. The internal inhibitor DB consists, for example, of members of the prominent class of WIN compounds, where typically a central phenoxy group (ring B) is separated from an isoxazole (ring C) by an aliphatic chain and is connected to another aromatic ring by a single bond (ring A) (Chart 1),<sup>1</sup> some larger Sandoz compounds containing up to four, often annelated, rings<sup>5,15</sup> and smaller compounds such as R 61837 (**3**), which is made up of three six-membered rings linked via single bonds.<sup>16</sup> Examples of these inhibitor classes can be seen in Chart 2 (compounds **2–11**). For the test set molecules conformational models representing their available conformational space were calculated. We selected the *best* quality option, an energy threshold of 20 kcal/mol above the lowest calculated



energy conformation, and a maximum number of 250 conformers.

Since the pharmacophore model generation was targeted at finding possible new leads for the HRV coat protein, we additionally screened other DBs such as the commercially available Maybridge DB. Its approximately 60 000 chemical compounds were registered as multiple conformers.

**Docking.** Docking presents a widely applied, computer-assisted approach to predict the 3D structure of protein–ligand complexes<sup>17</sup> and requires knowledge of the 3D structure of the target protein. By calculation of the steric and functional congruence of a particular molecule with the protein binding site, a prognosis regarding its biological activity is rendered possible. Docking can be applied for high-throughput virtual screening (HTVS) of large DBs as well as for docking single ligands into the binding site of interest. In the present study we employed the docking tool LigandFit implemented in the Cerius<sup>2</sup> software.

The LigandFit docking procedure includes i) a cavity detection algorithm to identify and select the region of the protein as the active site for docking and ii) the actual docking of the ligands to a selected site.<sup>18</sup> Finally, SFs allow evaluation and ranking of the compounds. The definition of the site, a set of unoccupied grid points, is based on the shape of the protein or, like in our study, on the structure of the ligand in complex with the protein binding site. Manual corrections of the defined binding site are possible. During the docking process several conformations of the molecules are taken into account. In Cerius<sup>2</sup> a broad coverage of conformational space of each molecule is achieved with a Monte Carlo based algorithm for conformation generation. While the molecules are treated as being flexible during docking, the protein is kept rigid. This common approximation is necessary in order to provide results within an acceptable time exposure. Finally, the ligands are docked and energy-minimized, and the best docked ligand structures according to a shape comparison with the site and the interaction possibilities are saved. Empirical, force field, or knowledge-based SFs pick out the binders against nonbinders and provide a ranking of the compounds and therefore an easier interpretation of the data. When the scores are computed, variable emphasis is placed on the influence of van der Waals and electrostatic terms. No generally applicable SF has been found so far, and so it is important to select a well-suited function for a particular biological target.<sup>19</sup> Another answer to this problem can be the calculation of a consensus score,<sup>20</sup> which makes use of the merits of different SFs by combining their results. For our docking approach we employed all SFs implemented in Cerius<sup>2</sup> (LigScore1, LigScore2,<sup>18,21</sup> PLP1, PLP2,<sup>22</sup> Jain,<sup>23</sup> PMF,<sup>24</sup> and Ludi<sup>25,26</sup>) as well as a consensus score thereof.

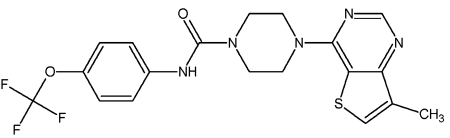
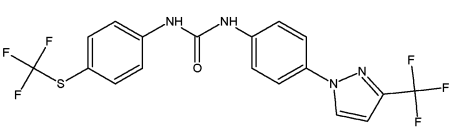
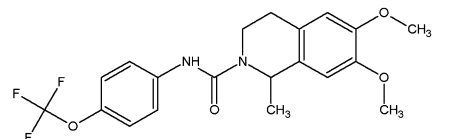
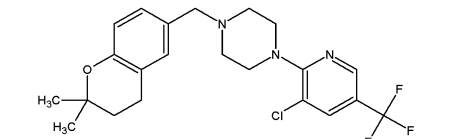
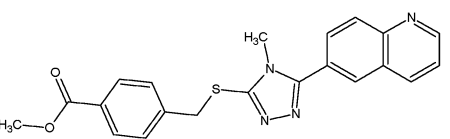
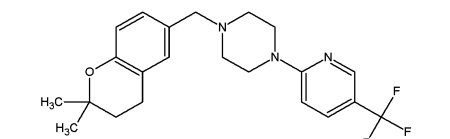
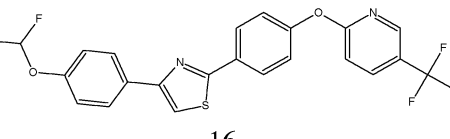
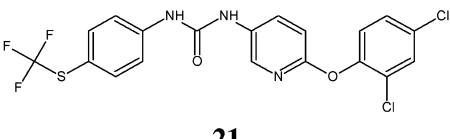
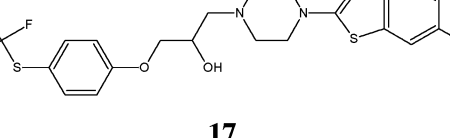
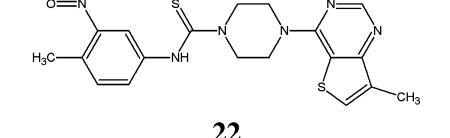
We present a two-step molecular docking strategy aimed at reviewing the resulting hits from pharmacophore DB screening by checking their proposed binding and interaction modes and by calculating estimated binding affinities with a suitable SF. First, an HTVS of a 1000-compound DB was carried out. The DB consists of 10 known HRV coat protein inhibitors (Chart 2) and 990 presumably inactive molecules randomly chosen

from a druglike virtual 10000-compound library generated with the program ilib diverse.<sup>27</sup> The ilib diverse software is a tool for fast creation of diverse virtual compounds and focused, combinatorial library generation. Two or more fragments are formally connected by the deletion of hydrogen atoms and the subsequent formation of new bonds. A selection of fragment sets, the desired number of fragments and molecular weight (MW) range, and the definition of atom reactivities guide the generation process. Finally, a filter system ensures reasonable chemical structures and druglikeness. The results of the docking process were analyzed in order to identify the best methodology (i.e., setting of parameters, selection of SF, and so on) for this target so that the active compounds are ranked at high positions in the resulting hit list and are retrieved in correct orientations and conformations compared to information from X-ray structures. In view of the second part of our docking procedure (the review of the molecules retrieved from screening the Maybridge DB with our pharmacophore model), this first step allows the setting of suitable docking and scoring conditions and increases reliability of the results. A final evaluation of these compounds in a small scale docking approach was achieved by judging their proposed binding modes and their calculated scores.

**Principal Component Analysis Based Clustering.** Since statistical methods have become essential to understand and analyze large volumes of biological and chemical data in QSAR work, Cerius<sup>2</sup> offers several data analysis, regression, and validation methods. PCA is a very popular data reduction technique. Its objective is to condense the information contained in a number of original variables into a smaller number of principal components without a significant loss of information.<sup>11</sup> For a set of molecules equipped with a selection of descriptors (molecular properties), trends and outliers can be detected. We applied a PCA-based clustering to find out whether the hits of the DB screening are clustered together with known active ligands, which would increase their chances of being active. Therefore, like the docking study, this approach aimed to validate and further refine and restrict the hit list obtained from pharmacophore model screening, the primary filtering tool. A set of descriptors was computed for the hits obtained from the Maybridge DB and 10 known HRV coat protein inhibitors (Charts 2 and 3). Cerius<sup>2</sup> provides a graphical representation of the PCA-based clustering results, where each structure is represented with a point in a 3D scores plot. In this way, similar compounds form clustered groupings of points, whereas those whose properties differ considerably from the others will be displayed by dispersed points.<sup>28</sup>

**In Vitro Anti-HRV Assay.** Compounds selected for the in vitro assay were ordered from the Maybridge DB. The purpose of this in vitro study was to determine if the Maybridge structures exhibited antiviral activity against rhinovirus. The assay was performed using HRV serotype 39, which belongs to the major group and utilizes ICAM-1 as cell receptor. The selected compounds were tested on two cell types: Ohio HeLa-I (OH-I) and human embryonic lung fibroblast cells (strain WI-38). The HRV 3C protease inhibitor rupintrivir (**12**) (Chart 1) served as a positive control.

**Chart 3.** Structures and Fit Values of 10 Compounds Retrieved from the Maybridge DB Using Hypo3 as Query Feature

Maybridge structure	Fit	Maybridge structure	Fit
	1.8		0.4
<b>13</b>		<b>18</b>	
	1.3		0.8
<b>14</b>		<b>19</b>	
	1.6		1.8
<b>15</b>		<b>20</b>	
	1.2		2.1
<b>16</b>		<b>21</b>	
	1.1		1.0
<b>17</b>		<b>22</b>	

The compounds were dissolved in DMSO at an initial concentration of 10 mg/mL except for GK 02681 (**13**), which did not dissolve in DMSO until the pH had been lowered for a final concentration of 9.9 mg/mL. All compounds were aliquoted and frozen at  $-70^{\circ}\text{C}$ . All molecule stocks were diluted subsequently in either 2% McCoy's for OH-I or 5% EMEM for WI-38 for a final concentration of 0.25% DMSO or 0.5% DMSO, respectively, for all compound concentrations.

Antiviral activity was determined by the previously described<sup>29,30</sup> multiple-cycle, cytopathic effect (CPE) inhibition assay in 96-well microtiter plates planted with 85% confluent OH-I and 100% confluent WI-38 monolayers with minor modifications. Triplicate monolayers were inoculated with 0.05 mL of media containing each compound immediately followed by 0.05 mL of three serial log dilutions of ATCC HRV serotype 39. The final compound concentrations were 100, 32, 10, 1, and 0.1  $\mu\text{g/mL}$  for OH-I cells and 32, 10, 3.2, 1.0, and 0.1  $\mu\text{g/mL}$  for WI-38 cells. A single drug concentration of the 3C protease inhibitor **12** at either 1.0 or 0.1  $\mu\text{g/mL}$  was used as a positive control. In addition, uninfected cell control monolayers, uninfected compound controls (three highest concentrations), DMSO control, and virus controls with a back titer of HRV serotype 39 were included on each microtiter plate. On day 3 and later, after inoculation, virus control monolayers were read

microscopically to determine when the virus control monolayers showed 80–100% CPE, and the amount of virus used in the inoculum contained 32–320 of median tissue culture infectious doses (TCID<sub>50</sub>). When these conditions are met, the plates were read microscopically for the degree of CPE inhibition in compound plus virus wells. Subsequently, the monolayers are stained with 0.1 mL of 0.4% crystal violet for 20–30 min at room temperature, rinsed with tap water five times, air-dried, and then destained with 0.1 mL of 30% methanol and 10% acetic acid for 15 min at room temperature. Plates with OH-I monolayers are read on a spectrophotometer at 550 nm. The WI-38 monolayers do not stain dark enough and are therefore only read microscopically. The inhibitory concentration (EC<sub>50</sub>) of the compound was defined as that causing a 50% increase in optical density compared to virus control. The formula for determining the percentage of compound inhibition is as follows:

$$\frac{[(\text{mean of OD of compound and virus}) - (\text{mean OD of virus control at 80–100\%})] - [(\text{mean of OD of negative control}) - (\text{mean of OD of virus control CPE})]}{(\text{mean of OD of virus control CPE})} \times 100$$

Then the EC<sub>50</sub> is calculated using the dose effect analysis with microcomputer software by Joseph Chou and Ting-Chao Chou.<sup>31,32</sup>

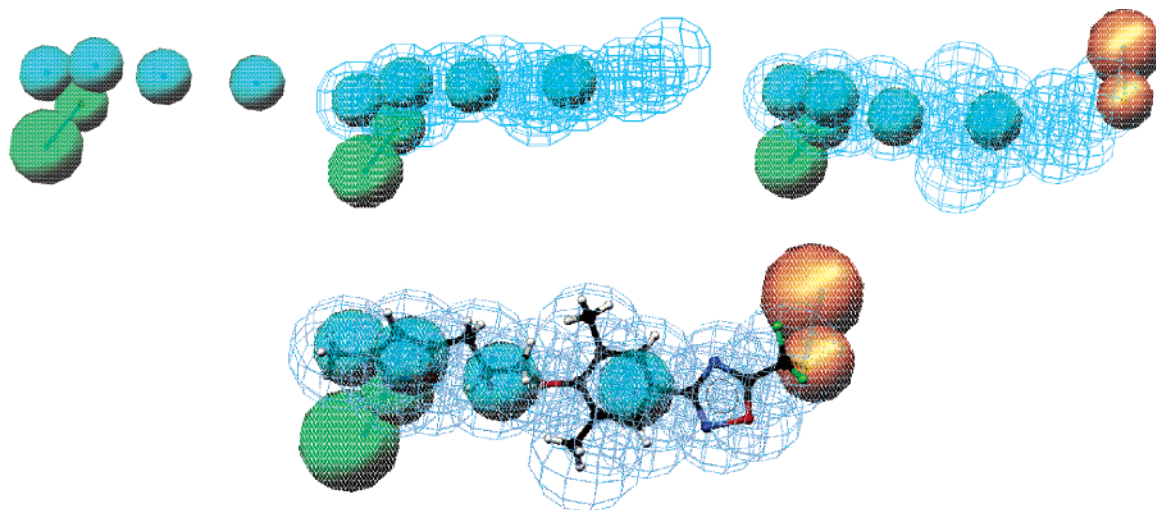


**Figure 1.** Structure-based pharmacophore hypotheses for HRV coat protein inhibitors built within the program Catalyst: Hypo1 (upper left), Hypo2 (upper middle), Hypo3 (upper right), and **2** mapped onto Hypo3 (lower illustration). Pharmacophore features are color-coded (green, HBA; orange, HBAF (customized function); cyan, H; blue, shape).

**Table 1.** Number and Percentage of Hits Retrieved with Three Structure-Based Hypotheses for HRV Coat Protein Inhibitors from an Internal Inhibitor Test Set, the Derwent WDI, and the Maybridge DB

hypothesis	test set	% of DB	Derwent WDI	% of DB	Maybridge DB	% of DB
Hypo1 (4 H, 1 HBA)	22	100.0	6836	14.1	8759	15.0
Hypo2 (4 H, 1 HBA, shape)	16	72.7	343	0.7	514	0.9
Hypo3 (4 H, 1 HBA, 1 HBAF, shape)	11	50.0	26	0.05	10	0.02

A static cytotoxicity test was performed on the two cell monolayers at or near 100% confluency for each compound at the three most concentrated compound strengths, ranging from 100 to 10  $\mu\text{g}/\text{mL}$  for OH-I or from 32 to 3.2  $\mu\text{g}/\text{mL}$  for WI-38 cells. If 50% or more of a monolayer is reduced compared to the cell control, that compound level is considered cytotoxic.

## Results and Discussion

**1. Hypothesis Generation and Database Screening.** The starting point for the hypothesis generation process was the PDB entry 1QJU<sup>1</sup> detected at a resolution of 2.8 Å, which contains HRV serotype 16 in complex with the highly active ligand WIN 61209 (**4**). The basic pharmacophore consists of four H features and one HBA, which hydrogen-bonds to Leu 100 via mediation by a water molecule. These features were placed manually on the corresponding groups of the ligand in its bioactive conformation, i.e., the isoxazole nitrogen, the phenyl ring, the methyl group, the propyl spacer, and the hydrophobic part of the isoxazole ring. The coordinates of the projected point of the vectorized HBA feature were taken from the X-ray information on the corresponding amino acid atom. This first model was called Hypo1 (Figure 1). Although this hypothesis was able to retrieve all members of our internal HRV coat protein inhibitor test set, it proved to be far too little restrictive to obtain utilizable results, i.e., small hit lists, when used for screening large DBs. Table 1 shows the performance of the different hypotheses in the 3D DB search. Since **4** fills the pocket quite nicely, a shape produced after this ligand accounting for the spatial restrictions of the protein was introduced as an additional feature into the pharmacophore hypothesis (Hypo2). Hypo2 (Figure 1) still identified more than 70% of the test set inhibitor molecules and resulted in only

343 hits from the Derwent WDI, which represents 0.7% of the entire DB. These hits were ranked according to their fit values. Thereby a calculation is performed to determine how well a compound fits a particular hypothesis, i.e., how well the ideal locations of the features can be matched by the corresponding functional groups of a molecule. The best 30 Derwent WDI compounds ranked on the basis of their fit values were studied. Among them, nearly two-thirds could be identified as already known rhinovirus capsid binders, proving the high quality of the model. However, using Hypo2 as query tool still retrieved too many structures from the Maybridge DB. From the binding mode of the furthest developed inhibitor **2** (Chart 2), an additional possibility for ligand–protein interaction was defined (PDB entries 1C8M, 1NCR): One fluorine atom of its trifluoromethyl group is within suitable distance of Tyr 144 to allow the formation of a hydrogen-bond-like electrostatic interaction. In the resulting Hypo3 (see Figure 1), this interaction is represented by a customized HBA whose definition had to be enlarged to also include fluorine atoms (HBAF).<sup>33</sup> Finally, with Hypo3 the required selectivity in DB screening could be achieved. We obtained a hit list of only 10 compounds from the Maybridge DB (see Chart 3, compounds **13–22**). Visual inspection and their fit values confirmed their good match with Hypo3. Additionally, their structures are analogous to the scaffold of known HRV coat protein inhibitors, namely, three to four ring systems consisting of a maximum of two annelated rings, which are connected to each other either directly or via aliphatic spacers. This common framework pattern is decisive for the ability of these compounds to perform antiviral activity at the HRV coat protein binding site. It guarantees a certain amount of flexibility, which not only enables the molecules to slip in the pocket through

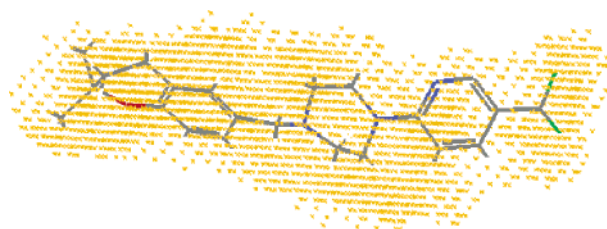


**Table 2.** Docking Scores Calculated for 10 Maybridge Compounds (Left) and 10 Known HRV Coat Protein Inhibitors (Right) Using the SF LigScore2 Implemented in the Software Cerius<sup>2</sup>

Maybridge hits	Conf_Number	LigScore2	HRV coat protein inhibitors	Conf_Number	LigScore2
16	3	7.14	10	3	7.48
17	3	7.13	10	1	7.04
17	5	7.09	10	9	6.91
14	1	7.04	9	4	6.83
13	4	7.03	6	3	6.43
16	2	7	10	8	6.40
17	10	7	9	3	6.36
18	1	6.98	9	5	6.32
18	4	6.93	2	1	6.31
15	1	6.91	6	1	6.3
21	4	6.9	9	8	6.28
15	2	6.88	8	6	6.28
15	3	6.86	6	4	6.24
16	5	6.86	7	1	6.16
16	1	6.8	4	3	6.07

a narrow pore on the bottom of the canyon but also allows stretched conformations required by the shape of the binding site. Therefore, these 10 compounds were seen fit to be subjected to further investigations.

**2. Docking. 2.1. HTVS for the Selection of the Best Suiting SF.** Three-dimensional structure information on the target protein was taken from the PDB entry 1C8M, detected at a resolution of 2.8 Å. Processing of the protein included the deletion of the ligand **2** and the solvent molecules as well as the addition of hydrogen atoms. The binding site was generated on the basis of the bound ligand. The site definition could be validated when **2** was docked back into the protein. The best docked pose judging from the calculated dockscore value differs only minimally from the position of the ligand retrieved from X-ray information expressed by a root-mean-square (rms) deviation of 0.5 Å. As outlined before, we were interested under which experimental conditions, especially with which SF, the LigandFit program would be able to retrieve 10 known active HRV coat protein inhibitors within a DB of 1000 diverse and druglike compounds by attributing top ranking scores to these molecules. The 10 active compounds, displayed in Chart 2, were extracted from PDB complexes (1C8M, 1QJU, 1QJY, 1R08, 1HRV, 1VRH, 1R09, 2RS3, 2RR1, and 2HWB) assigning random, minimized conformations to them. A large in-house DB of 10 000 compounds generated with the software ilib diverse 0.6 was the source for the presumably inactive molecules. The druglike molecules were generated, each starting from four fragments, and a MW between 200 and 700 was requested. For our HTVS approach, a diverse set of 990 of these druglike structures, by all probability inactive, were randomly chosen and united with the 10 known inhibitors. For all ligand structures partial charges were automatically assigned using the Gasteiger calculation implemented in the Cerius<sup>2</sup> docking process. All 1000 molecules were flexibly docked employing the CFF force field for energy minimization and charge calculations. The number of maximum trials was set to 5000, the number of saved conformations was set to 20, and the grid resolution was set to 0.5 Å. Other parameters remained at their default values. Only 753 molecules could be docked into the site, leading to a total of 8645 poses. Scores for the molecules were computed using the following SFs: LigScore1, LigScore2, PLP1, PLP2, Jain, PMF, Ludi, and consensus score. Analyzing the retrieved hit lists revealed that LigScore2 performs best

**Figure 2.** Maybridge compound **20** docked into the binding site.

in ranking the active molecules at high positions. Among the first ranked 76 structures, nine active ones could be found. Furthermore, 80% were orientated correctly in the binding site, and the rms deviations between their docked and their X-ray conformations were less than 1.5 Å. Other SFs and also consensus scoring performed considerably worse. On the basis of these results, LigScore2, a SF whose descriptors represent van der Waals interactions as well as the influence of the buried polar surface between the ligand and the protein,<sup>21</sup> is best suited for this biological system and was therefore applied for reviewing the Maybridge hits.

**2.2. Review of the Maybridge Compounds.** Ten compounds from the Maybridge DB (Chart 3) retrieved via the pharmacophore hypothesis DB screening procedure were submitted to a docking and scoring process using the same experimental conditions, which had achieved the best results in the HTVS study. Inspection of the docked structures shows that some of the compounds fit the binding site very well and can be perfectly overlaid with inhibitor **2** in its bound conformation (see Figures 2 and 3). Also, the calculated LigScore2 values for the best compounds and conformations were in good agreement with the values retrieved for the active inhibitors used in the HTVS experiment (Table 2). Figures 4 and 5 illustrate exemplarily the putative binding modes of two docked Maybridge compounds. For HTS-05932 (**14**) the pattern of hydrogen bonding is analogous to **2**; the oxygen atom of one of the methoxy residues accepts a hydrogen bond from Leu 100, a crucial amino acid for inhibitor binding in this site, and the trifluoromethyl group functions as HBAF for Tyr 144. Additionally, another possibility for interaction evolves from the proximity of the second methoxy group of the ligand to the side chain nitrogen atom of Asn 212. In compound KM 10639 (**15**) the favorable orientation of the carbonyl oxygen atom enables hydrogen bonds



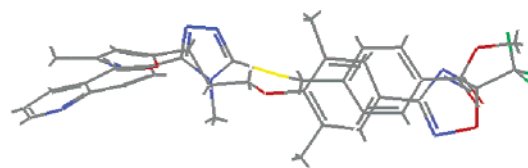
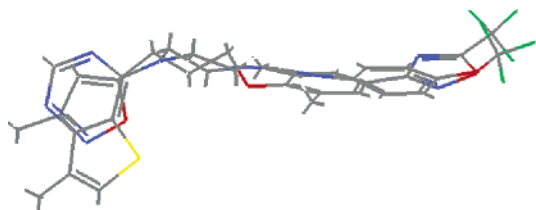


**Figure 3.** Docked structures of Maybridge compound **13** (left) and **15** (right) overlaid with protein-bound conformation of **2**.

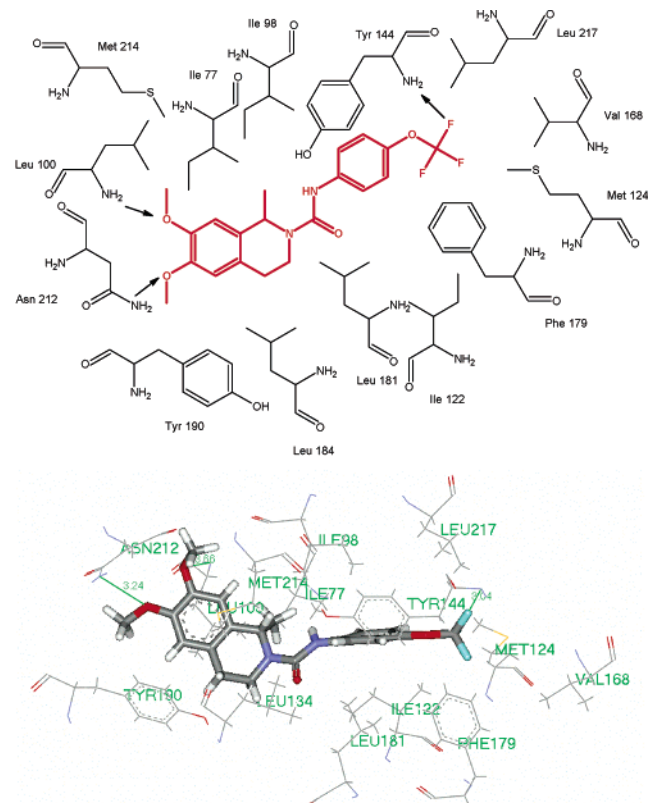


**Figure 4.** Putative binding mode of Maybridge compound **14** docked into HRV coat protein binding site. Possibilities of interaction with the surrounding amino acids include three hydrogen bonds as well as several hydrophobic contacts.

with the same amino acids at the pocket entry, i.e., Leu 100 and Asn 212. In contrast to most of the WIN compounds, this potential ligand can interact with a residue in the central part of the binding site, namely, Ser 120, via its sulfur atom. The concept of an advantageous hydrogen bond in this region has already been realized in other prominent HRV coat protein inhibitors such as SDZ 35-682 (**5**) (PDB entry 1HRV). Aside from these directed polar interactions the predominantly hydrophobic character of the pocket reveals hydrophobic contacts as a major driving force for ligand binding. Both Maybridge compounds fulfill this requirement because the lipophilic parts of their scaffolds are situated at a suitable distance from hydrophobic amino acid side chains, e.g., of leucines 100, 181, 184, and 217, isoleucines 77, 98, 122, and 236, methionines 124 and 214, and the aromatic moieties of Tyr 144, Phe 179, and Phe 190.

According to the insights of this docking approach, we considered that especially compounds **13–15**, SP 00704 (**16**), AW 00641 (**17**), HAN 00352 (**18**), HTS 05408 (**19**), and HTS 05404 (**20**) have a high probability of displaying biological activity.

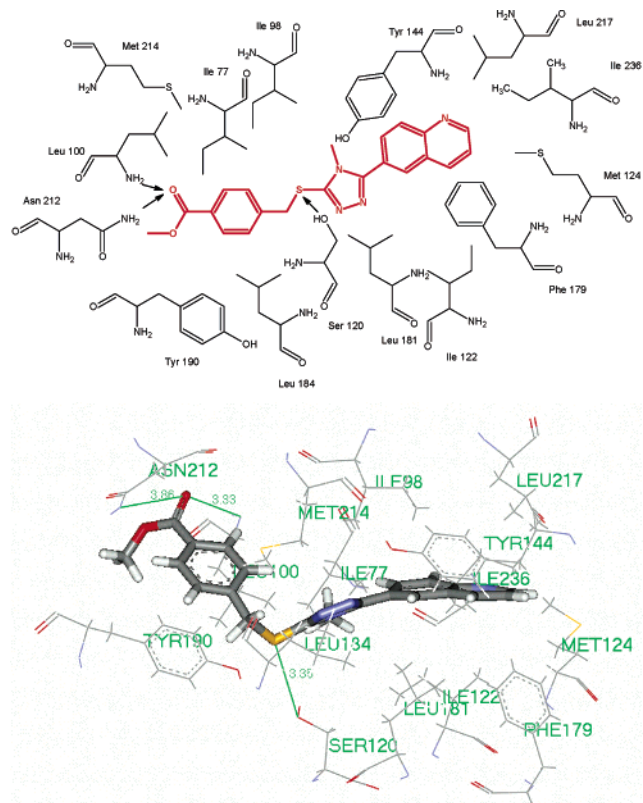


**Figure 5.** Putative binding mode of Maybridge compound **15** docked into HRV coat protein binding site. Possibilities of interaction with the surrounding amino acids include three hydrogen bonds as well as several hydrophobic contacts.

**3. Principal Component Analysis Based Clustering.** The data set consisted of the 10 hits retrieved from the Maybridge DB as well as 10 structurally diverse, known HRV coat protein inhibitors identical to those used for the HT docking approach (see Charts 2 and 3). A total of 34 descriptors, listed in Table 3, were calculated within Cerius<sup>2</sup> for these 20 compounds to outline their property profiles as extensively as possible. The descriptors included AlogP98, violations of the rule of five, HBD and HBA qualities, MW, number of rotatable bonds, and several topological parameters.<sup>34</sup> The data were saved in binary data file format and submitted to PCA. For easier interpretability of the results, a 3D plot display style was chosen. Figure 6 shows this 3D plot of the 20 compounds distributed across property space. The molecules were clustered together accounting for their similarity. The idea was to estimate whether the hits from DB screening conform to known active inhibitors that obviously possess suitable qualities for biological activity. In other words, outlying hit structures would obtain lower priority when selecting substances for further investigations, e.g., biological evaluation. Red color coding of the Maybridge compounds proved that they were continuously distributed among the known

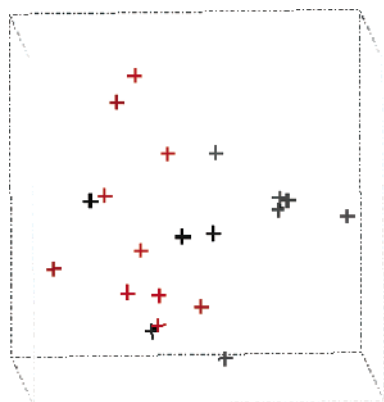
**Table 3.** Fast Descriptor Set for PCA-Based Clustering of 10 Known HRV Coat Protein Inhibitors and 10 Hits from the Maybridge DB<sup>34,40–43</sup>

family	descriptor	descriptor assembly
structural	MW	
structural	Rotlbonds	
structural	hydrogen bond acceptor	
structural	hydrogen bond donor	
thermodynamic	AlogP98	
ADME	violations of rule of five	
topological	Zagreb	
topological	$\chi$ indices	CHI-0, CHI-1, CHI-2, CHI-3_P, CHI-3_C, CHI-3_CH, CHI-V-0, CHI-V-1, CHI-V-2, CHI-V-3_P, CHI-V-3_C, CHI-V-3_CH
topological	$\kappa$ indices	$\kappa$ -1, $\kappa$ -2, $\kappa$ -3, $\kappa$ -1-AM, $\kappa$ -2-AM, $\kappa$ -3-AM
topological	Balaban	JX
topological	SubgraphCount	SC-0, SC-1, SC-2, SC-3_P, SC-3_C, SC-3_CH
topological	Wiener	
topological	PHI	

**Table 4.** Experimental EC<sub>50</sub> Values of the Six Maybridge Compounds for the Major Group HRV Serotype 39 on OH-I and WI-38 Cells

Maybridge hits	EC <sub>50</sub> , $\mu\text{mol/L}$ ( $\mu\text{g/mL}$ ) OH-I microscopic	EC <sub>50</sub> , $\mu\text{mol/L}$ ( $\mu\text{g/mL}$ ) OH-I spectrophotometric	EC <sub>50</sub> , $\mu\text{mol/L}$ ( $\mu\text{g/mL}$ ) WI-38 microscopic
<b>13</b>	7.3 (3.2)	4.3 (1.9)	48.0 (21.0)
<b>14</b>	120.6 (49.5)	4.9 (2.0) <sup>a</sup>	<78.0 (<32)
<b>15</b>	142.4 (55.6)	88.4 (34.5)	<82.0 (<32)
<b>18</b>	247.1 (110.3)	245.5 (109.6)	11.2 (5.0)
<b>19</b>	35.7 (15.7)	32.1 (14.1)	<72.7 (<32)
<b>20</b>	15.0 (6.1)	17.0 (6.9)	165.0 (66.9)

<sup>a</sup> This result is not accurate because a lot of undissolved compound crystals were present at 100 and 32  $\mu\text{g/mL}$  and were stained, creating a false reading at those concentrations.

**Figure 6.** 3D plot displaying the results of a PCA-based clustering for 10 HRV coat protein inhibitors (grey) and 10 hits from the Maybridge DB (red) using a set of 34 descriptors.

inhibitors, and no extreme outliers could be observed. Nevertheless, three molecules, **16**, **17**, and BTB 08360 (**21**), were identified that are situated a bit more separated from the cluster and therefore evidently possess lower molecule property similarity. This makes them less favorable candidates for biological testing.

The same experimental setup for PCA-based clustering had been applied beforehand to analyze the property conformity of the test DB consisting of 990 presumably inactive and 10 known active compounds used to identify the best-suited docking and scoring conditions as described in Docking. Thereby, the majority of the inactive molecules were found to be accumulated with the active substances confirming the appropriateness of the DB.

Finally, the combined results of these virtual screening and evaluation approaches enabled the selection of six promising structures: **13–15** and **18–20**. They excelled the others in their overall performance (their

match with the pharmacophore hypothesis (fit values), the docking and scoring results, and their behavior in the PCA-based clustering) and were therefore submitted to biological testing.

**4. Biological Data.** The ability of the selected compounds to inhibit HRV serotype 39 was evaluated as reported in the General Methodology. The biological results determined by multiple-cycle CPE inhibition assay and expressed as EC<sub>50</sub> values are reported in Table 4. Microscopic and spectrophotometric reading confirmed that all of the six Maybridge compounds inhibit viral growth on OH-I and WI-38 cells and show activities in the micromolar range. This means that at this level of activity we could achieve a success rate of 100% in the selected hit list. Particularly promising results were achieved for compound **13**, which shows an EC<sub>50</sub> of 4.3  $\mu\text{M}$  for OH-I cells and also for compound **20**, which inhibits the virus at a concentration of approximately 15  $\mu\text{M}$ . For the Maybridge substances, favorable druglike profiles had been anticipated beforehand with the aid of the druglikeness and molecular property prediction tool MolSoft, and except for one structure, **18**, whose log *P* value slightly exceeds the cutoff value of 5, all candidates conform to the “Lipinski rule of five”.<sup>35–37</sup> Despite this preliminary inquiry, difficulties complicating the interpretation of the assay results arose from the relatively high cytotoxicity of the compounds and the fact that some of them precipitated out of solution. This demonstrates the necessity for more cautious estimation of molecular properties, especially toxicity and solubility, for future compound selection. On the other hand, the efficiency of the described workflow itself, combining virtual screening tools to identify structures with potential inhibitory activity for the HRV coat protein, could be clearly shown by the high success rate retrieved in the biological assay and does not conflict with the observed toxicity.

**4.1. Cytotoxicity.** A static toxicity test was performed on the different monolayers at or near 100% confluency for each compound at the three most concentrated dilutions, ranging from 100 to 10  $\mu\text{g}/\text{mL}$  for OH-I or from 32 to 3.2  $\mu\text{g}/\text{mL}$  for WI-38 cells. If 50% or more of a monolayer is reduced compared to the cell control, that compound level is considered cytotoxic.

On OH-I monolayers, **13**, **14**, and **18** exhibited 50–100% cellular toxicity at 100, 32, and 10  $\mu\text{g}/\text{mL}$ . At 100 and 32  $\mu\text{g}/\text{mL}$ , **19** and **20** exhibited 50–100% toxicity and each demonstrated a 30% toxic effect at 10  $\mu\text{g}/\text{mL}$ . Compound **15** produced a 30% toxic effect at 100  $\mu\text{g}/\text{mL}$ . The WI-38 monolayer reduced the toxic effect; only **18** produced toxicity at 32 and 10  $\mu\text{g}/\text{mL}$  of  $\leq 50\%$ . For comparison, when **2** and **12** were tested under similar conditions for both compounds, altered cellular morphology was observed in uninfected control cells at the highest concentration tested (100  $\mu\text{g}/\text{mL}$ ). The median cytostatic concentration, even though for growing cells, was 30.0  $\mu\text{g}/\text{mL}$  for **2** and  $>100$   $\mu\text{g}/\text{mL}$  for **12**.<sup>38</sup>

**4.2. Antiviral Activity.** Two compounds that exhibited approximately 30% toxicity demonstrated inhibitory effects on OH-I monolayers: **15** at 100  $\mu\text{g}/\text{mL}$  but no inhibition at 32  $\mu\text{g}/\text{mL}$ , meaning a 3-fold effect, and **20** at 10  $\mu\text{g}/\text{mL}$  but no inhibition at 1  $\mu\text{g}/\text{mL}$ , which amounts to a 10-fold effect. For structures **13**, **14**, **18**, and **19** virus inhibition occurred only at concentrations beyond 50% toxicity. The positive control **12** was inhibitory at 1.0  $\mu\text{g}/\text{mL}$ . The CPE inhibition test on OH-I monolayers had a final DMSO concentration of 0.25% for all compound concentrations. The 0.25% DMSO level caused **13–15** and **20** to precipitate out of solution as crystals at 100  $\mu\text{g}/\text{mL}$  and all except **20** at 32  $\mu\text{g}/\text{mL}$ .

On WI-38 monolayers compounds **13** and **20** each exhibited a 3-fold antiviral effect or inhibition at 32  $\mu\text{g}/\text{mL}$  but none at 10  $\mu\text{g}/\text{mL}$ . At the highest concentration of 32  $\mu\text{g}/\text{mL}$ , **14**, **15**, and **19** showed no antiviral effect. The antiviral activity of **18** lay beyond the toxic levels of 32 and 10  $\mu\text{g}/\text{mL}$ . The positive control **12** was inhibitory at 0.1  $\mu\text{g}/\text{mL}$ .

Structural analyses reveal the following aspects: In contrast to the other structures investigated in the assay, **15** does not possess a trifluoromethyl substituent but rather matches the hydrophilic inner part of the binding site, i.e., the HBAF feature in the pharmacophore hypothesis, with the carbonyl oxygen of its methyl ester group. Compared to the most active compound **13**, it displays an approximately 20-fold lower inhibitory activity. A double trifluoromethyl substitution is present in **18**. The latter was found to be active against rhinovirus on WI-38 monolayers with an  $\text{EC}_{50}$  of 11.2  $\mu\text{M}$  but is disadvantageous because of its high cellular toxicity. It is worth mentioning the differences between the behavior of **20** and its analogue **19**. The additional chlorine substitution at the pyridine ring of **19** obviously not only provokes a loss in activity (35.7  $\mu\text{M}$  for **19** versus 15.0  $\mu\text{M}$  for **20**) but also a much more unfavorable toxicologic profile.

Maybridge substance **20** on both monolayers of OH-I and WI-38 exhibited antiviral potential of 10- and 3-fold inhibitory effect difference between viral and cellular inhibitory concentrations. Furthermore, **13** on WI-38 and **15** on OH-I produced a 3-fold inhibitory effect. Since these three structures display the most beneficial ratios

between inhibitory activity and cellular toxicity, they can be considered the most promising candidates of our selection. Whereas the observed rather unfavorable property profiles of the Maybridge substances cast their direct applicability in lead generation into doubt, the enormous value for model validation is unquestionable and it characterizes them as typical chemical tools.<sup>39</sup>

## Conclusions

The development of a successful virtual screening and selection protocol is described. The latter underwent thorough theoretical and practical validation and is aimed at enabling the fast and reliable identification of potential new inhibitors of the HRV coat protein. The main challenge was to achieve hit lists in which the likelihood that the selected compounds display the desired affinity is increased. Therefore, a combination of virtual techniques was employed. We could show that a highly selective pharmacophore model, used to screen and considerably reduce large 3D DBs, and the following validation and refinement of the obtained results via docking and PCA-based clustering lead to an enrichment of actives in the selected compound list. Six compounds from the Maybridge DB were chosen and underwent exemplary biological testing against one major receptor group virus serotype. All of the molecules displayed antirhinoviral activity in the micromolar range representing a hit rate of 100%. It can be concluded that such a rational approach increases the efficiency in identifying novel active structures and can help to reduce time and cost-intensive steps in the drug development process.

## Experimental Section

All molecular modeling studies were performed using Catalyst 4.7 and Cerius<sup>2</sup> 4.8 installed on a Silicon Graphic Octane desktop workstation equipped with a 300 MHz MIPS R12000 processor (512 MB RAM) running the Irix 6.5 operating system.

**Acknowledgment.** We thank Dr. Rémy Hoffmann (Accelrys SARL, Paris) for performing the screening of the Derwent WDI.

## Appendix

**Abbreviations.** ICAM-1, intercellular adhesion molecule-1; HRV, human rhinovirus; PDB, Brookhaven Protein Databank; PCA, principal component analysis; DB, database; SF, scoring function; HBA, hydrogen bond acceptor; HBD, hydrogen bond donor; H, hydrophobic feature; WDI, World Drug Index; HTVS, high-throughput virtual screening; HBAF, fluorine atoms including hydrogen bond acceptor; MW, molecular weight; OH-1, Ohio HeLa-1; WI-38, human embryonic lung fibroblasts;  $\text{TCID}_{50}$ , median tissue culture infectious doses; CPE, cytopathic effect;  $\text{EC}_{50}$ , 50% inhibitory concentration; rms, root-mean-square.

## References

- (1) Hadfield, A. T.; Diana, G. D.; Rossmann, M. G. Analysis of three structurally related antiviral compounds in complex with human rhinovirus 16. *Proc. Natl. Acad. Sci. U.S.A.* **1999**, *96*, 14730–14735.
- (2) Kolatkar, P. R.; Bella, J.; Olson, N. H.; Bator, C. M.; Baker, T. S.; et al. Structural studies of two rhinovirus serotypes complexed with fragments of their cellular receptor. *EMBO J.* **1999**, *18*, 6249–6259.



- (3) Hayden, F. G.; Herrington, D. T.; Coats, T. L.; Kim, K.; Cooper, E. C.; et al. Efficacy and safety of oral pleconaril for treatment of colds due to picornaviruses in adults: results of 2 double-blind, randomized, placebo-controlled trials. *Clin. Infect. Dis.* **2003**, *36*, 1523–1532.
- (4) Hayden, F. G.; Coats, T.; Kim, K.; Hassman, H. A.; Blatter, M. M.; et al. Oral pleconaril treatment of picornavirus-associated viral respiratory illness in adults: efficacy and tolerability in phase II clinical trials. *Antiviral Ther.* **2002**, *7*, 53–65.
- (5) Rosenwirth, B.; Oren, D. A.; Arnold, E.; Eggers, H. J. SDZ 35-682, a new picornavirus capsid-binding agent with potent antiviral activity. *Antiviral Res.* **1995**, *26*, 65–82.
- (6) Brookhaven Protein Data Bank ([www.rcsb.org/pdb/](http://www.rcsb.org/pdb/)).
- (7) Farber, G. K. New approaches to rational drug design. *Pharmacol. Ther.* **1999**, *84*, 327–332.
- (8) Böhm, H. J.; Klebe, G.; Kubinyi, H. *Wirkstoffdesign* (Active Substance Design); Spektrum Akademischer Verlag GmbH: Heidelberg, Berlin, Oxford, 1996.
- (9) *Catalyst*, version 4.7, Accelrys Inc.: San Diego, CA; <http://www.accelrys.com>.
- (10) *Maybridge Organic Chemical Catalog*, 62000 Compounds.
- (11) Migliavacca, E. Applied introduction to multivariate methods used in drug discovery. *Mini-Rev. Med. Chem.* **2003**, *3*, 831–843.
- (12) *Cerius<sup>2</sup>*, version 4.8, Accelrys Inc.: San Diego, CA; <http://www.accelrys.com>.
- (13) Kubinyi, H. Drug research: myths, hype and reality. *Nat. Rev. Drug Discovery* **2003**, *2*, 665–668.
- (14) Derwent World Drug Index, <http://thomsonderwent.com/products/lr/wdi/>; available in the Catalyst software package, Thompson Derwent.
- (15) Oren, D. A.; Zhang, A.; Nesvadba, H.; Rosenwirth, B.; Arnold, E. Synthesis and Activity of piperazine-containing antirhinoviral agents and crystal structure of SDZ 880-061 bound to human rhinovirus 14. *J. Mol. Biol.* **1996**, *259*, 120–134.
- (16) Chapman, M. S.; Minor, I.; Rossmann, M. G.; Diana, G. D.; Andries, K. Human rhinovirus 14 complexed with antiviral compound R 61837. *J. Mol. Biol.* **1991**, *217*, 455–463.
- (17) Muegge, I.; Rarey, M. Small molecule docking and scoring. *Rev. Comput. Chem.* **2001**, *17*, 1–60.
- (18) Venkatachalam, C. M.; Jiang, X.; Oldfield, T.; Waldman, M. LigandFit: A novel method for the shape-directed rapid docking of ligands to protein active sites. *J. Mol. Graphics Modell.* **2003**, *21*, 289–307.
- (19) Kontoyianni, M.; McClennan, L.; Sokol, G. Comparative evaluation of docking performance and library ranking efficacy. Presented at the 36th Middle Atlantic Regional Meeting of the American Chemical Society, Princeton, NJ, June 8–12, 2003.
- (20) Clark, R. D.; Strizhev, A.; Leonard, J. M.; Blake, J. F.; Matthew, J. B. Consensus scoring for ligand/protein interactions. *J. Mol. Graphics Modell.* **2002**, *20*, 281–295.
- (21) Venkatachalam, C. M.; Krammer, A.; Waldman, M. New developments in protein–ligand scoring functions: LigScore2 and LigScore3. *Abstracts of Papers*, 227th National Meeting of the American Chemical Society, Anaheim, CA; American Chemical Society: Washington, DC, 2004.
- (22) Gehlhaar, D. K.; Verkhivker, G. M.; Rejto, P. A.; Sherman, C. J.; Fogel, D. B.; et al. Molecular recognition of the inhibitor AG-1343 by HIV-1 protease: Conformationally flexible docking by evolutionary programming. *Chem. Biol.* **1995**, *2*, 317–324.
- (23) Jain, A. N. Scoring noncovalent protein–ligand interactions: A continuous differentiable function tuned to compute binding affinities. *J. Comput.-Aided Mol. Des.* **1996**, *10*, 427–440.
- (24) Muegge, I.; Martin, Y. C. A general and fast scoring function for protein–ligand interactions: A simplified potential approach. *J. Med. Chem.* **1999**, *42*, 791–804.
- (25) Böhm, H. J. The development of a simple empirical scoring function to estimate the binding constant for a protein–ligand complex of known three-dimensional structure. *J. Comput.-Aided Mol. Des.* **1994**, *8*, 243–256.
- (26) Böhm, H. J. Prediction of binding constants of protein ligands: a fast method for the prioritization of hits obtained from de novo design or three-dimensional database search programs. *J. Comput.-Aided Mol. Des.* **1998**, *12*, 309–323.
- (27) *ilib diverse*, version 1.0, Inte:Ligand GmbH: Maria Enzersdorf, Austria; [www.inteligand.com](http://www.inteligand.com).
- (28) Jamois, E. A. *Analysis of Multiple QSAR Models. Unleashing the Power of GFA*; Accelrys Inc.: San Diego, CA, 2003.
- (29) Arruda, E.; Crump, C. E.; Marlin, S. D.; Merluzzi, V. J.; Hayden, F. G. In vitro studies of the antirhinovirus activity of soluble intercellular adhesion molecule-1. *Antimicrob. Agents. Chemother.* **1992**, *36*, 1186–1191.
- (30) Andries, K.; Dewindt, B.; De Brabander, M.; Stokbroekx, R.; Janssen, P. A. In vitro activity of R 61837, a new antirhinovirus compound. *Arch. Virol.* **1988**, *101*, 155–167.
- (31) Chou, T.-C.; Talalay, P. Analysis of combined drug effects: A new look at a very old problem. *Trends Pharmacol. Sci.* **1983**, *4*, 450–454.
- (32) *Biosoft Package: Dose Effect Analysis with Microcomputers*; Biosoft: Cambridge, U.K.; [www.biosoft.com](http://www.biosoft.com).
- (33) Böhm, H. J.; Banner, D.; Bendels, S.; Kansy, M.; Kuhn, B.; et al. Fluorine in Medicinal Chemistry. *ChemBioChem.* **2004**, *5*, 637–643.
- (34) *Cerius<sup>2</sup>*, version 4.8, *Documentation, QSAR, 4. Theory: QSAR + Descriptors*; Accelrys Inc.: San Diego, CA; <http://www.accelrys.com>.
- (35) Sander, T. *OSIRIS Property Explorer*; Actelion: Allschwil, Switzerland; <http://www.organic-chemistry.org/prog/peol/>.
- (36) MolSoft LLC: La Jolla, CA; <http://www.molsoft.com/mprop/>.
- (37) Lipinski, C. A.; Lombardo, F.; Dominy, B. W.; Feeney, P. J. Experimental and computational approaches to estimate solubility and permeability in drug discovery and development settings. *Adv. Drug. Delivery Rev.* **1997**, *23*, 3–25.
- (38) Kaiser, L.; Crump, C. E.; Hayden, F. G. In vitro activity of pleconaril and AG7088 against selected serotypes and clinical isolates of human rhinoviruses. *Antiviral Res.* **2000**, *47*, 215–220.
- (39) Lipinski, C. A. Lead- and drug-like compounds: the rule-of-five revolution. *Drug Discovery Today: Technol.* **2004**, *1*, 337–341.
- (40) Rogers, D.; Hopfinger, A. J. Application of genetic function approximation to quantitative structure–activity relationships and quantitative structure–property relationships. *J. Chem. Inf. Comput. Sci.* **1994**, *34*, 854–866.
- (41) Rohrbaugh, R. H.; Jurs, P. C. Descriptions of molecular shape applied in studies of structure/activity and structure/property relationships. *Anal. Chim. Acta* **1987**, *199*, 99–109.
- (42) Hall, L. H.; Kier, L. B. Molecular connectivity chi indices for database analysis and structure–property modeling. *Topol. Indices Relat. Descriptors QSAR QSPR* **1999**, 307–360.
- (43) Stanton, D. T.; Jurs, P. C. Development and use of charged partial surface area structural descriptors in computer-assisted quantitative structure–property relationship studies. *Anal. Chem.* **1990**, *62*, 2323.

JM050343D